

Contents lists available at ScienceDirect

Carbon

journal homepage: www.elsevier.com/locate/carbon



Large-scale cellulose-assisted transfer of graphene toward industrial applications



Mingguang Chen ^{a, d}, Guanghui Li ^{a, d}, Wangxiang Li ^{b, d}, Dejan Stekovic ^{b, d}, Bassim Arkook ^{c, d}, Mikhail E. Itkis ^{a, b, c, d}, Aron Pekker ^{b, d}, Elena Bekyarova ^{a, b, c, d, *}, Robert C. Haddon ^{a, b, c, d, **}

- ^a Department of Chemical and Environmental Engineering, University of California, Riverside, CA 92521, United States
- ^b Department of Chemistry, University of California, Riverside, CA 92521, United States
- ^c Department of Physics, University of California, Riverside, CA 92521, United States
- ^d Center for Nanoscale Science and Engineering, University of California, Riverside, CA 92521, United States

ARTICLE INFO

Article history: Received 13 August 2016 Received in revised form 9 September 2016 Accepted 12 September 2016 Available online 13 September 2016

ABSTRACT

CVD graphene has attracted a great deal of interest from both academia and industry. The strong motivation to commercialize high quality CVD graphene films and related devices has been restricted by the lack of a cheap, efficient, clean and reliable graphene transfer process. In this article, we report a novel graphene transfer technique which provides a route to high-throughput, reliable and economical transfer of graphene without introducing large cracks and residue contamination from polymers, such as PMMA or magnetic impurities. The transferred graphene was thoroughly characterized with Raman spectroscopy, Atomic Force Microscopy, and X-ray photoelectron spectroscopy. Fabricated large area graphene-based field effect transistors exhibited high mobilities, which were about 2 times higher than those for devices prepared with graphene transferred by the conventional wet transfer method. This new graphene transfer technique has the potential to expedite the large scale industrial utilization of CVD graphene in electronics, spintronics, catalysis and energy storage.

© 2016 Elsevier Ltd. All rights reserved.

1. Introduction

Graphene is a one atom thick two dimensional carbon material, whose valence and conduction bands touch each other at the Dirac point [1,2]. The fascinating properties, which originate from the unique electronic structure of graphene, motivate the wide interest in its potential application in many fields, such as electronics [3–8], spintronics [9], optics [5], environmental engineering [10,11], and aerospace [12]. Chemical vapor deposition (CVD) is among the most promising methods for production of macro-size, continuous, high-quality graphene films for industrial applications [13–16].

The first step in the fabrication of devices based on CVD graphene is transfer of the as-grown graphene from copper or nickel to a targeted substrate, usually SiO₂/Si, boron nitride, or quartz.

E-mail address: elanab@ucr.edu (E. Bekyarova).

Although several transfer methods have been developed so far, few can be used for industrial applications due to their timeconsuming, costly, or challenging scalability [17,18]. A conventional graphene wet transfer method [13,14] widely employed in academia utilizes poly(methyl methacrylate) (PMMA) as the supporting layer and etching of the Cu or Ni substrate with iron chloride or iron nitrate [19–22]. However, researchers have been struggling with the degradation of graphene's intrinsic properties by contaminations from residues of PMMA and paramagnetic Fe³⁺ [23-25]. Few advances have been made towards a highthroughput economic transfer of graphene for commercialization needs. Although the roll-to-roll (R2R) method can transfer large scale graphene onto targeted substrates [16,26], the thermal release tape is known to leave contamination on the graphene layer [14,27] and R2R method is not applicable to SiO₂/Si substrates, limiting its application in the semiconductor industry. The face-to-face graphene transfer method offers large-area, continuous graphene films with reduced density of transfer defects, however, the process is designed for "stiff" substrates [17]. The clean lifting transfer (CLT) method solved the issue of PMMA residue by making use of an

^{*} Corresponding author. Center for Nanoscale Science and Engineering, University of California, Riverside, CA 92521, United States.

^{**} Corresponding author. Center for Nanoscale Science and Engineering, University of California, Riverside, CA 92521, United States.

electrostatic attraction force to protect graphene during the transfer process. However, this method uses high voltage and it has a strict requirement for the surface flatness of the as-grown graphene on Cu or Ni, which restrict its potential industrial application. Additionally, the contamination with paramagnetic Fe³⁺ remains an unresolved issue. For transfer methods that employed ammonium persulfate as the etching solution in order to avoid contamination from paramagnetic materials [28–30], the cost and time increased dramatically.

In this article, we discuss the development of a novel technique for the transfer of graphene on various substrates. The method utilizes cellulose acetate as the coating layer, which protects graphene from unfavourable forces and contaminations during the transfer process by forming a soft flexible thin film on top of graphene. The etching of Cu foil, used in the CVD graphene growth, is accomplished with a hydrogen peroxide – hydrogen chloride solution, which decreases the possibility for magnetic contamination of the graphene. This cellulose assisted transfer (CAT) method largely reduces the cost, time and contaminations of the obtained graphene layer and can be expanded to industrial scale applications. The main advantages of the CAT method in comparison with other graphene transfer techniques are summarized in Table 1. The transferred grapene films were characterized with Raman spectroscopy, atomic force microscopy (AFM) and X-ray photoelectron spectroscopy (XPS) to evaluate the quality of the obtained films. The fabricated field effect transistor (FET) devices showed high mobility and high on-off ratio.

2. Experimental

2.1. CAT graphene transfer

As-grown monolayer CVD graphene (Graphene Supermarket) was first spin coated with a cellulose acetate solution (Average Mn ~ 50,000 by GPC, Sigma Aldrich, 4.5 mg/mL dissolved in acetone) at 2000 rpm. The spin-coated thin film dries immediately as the acetone evaporates. The graphene on the uncoated side was etched away by oxygen plasma (Oxford Plasmalab 100/180 model; forward power 30 W; ICP power 300 W, etching time 30 s). An aqueous solution of H₂O₂ and HCl was prepared by mixing equal volumes of 2 M HCl and 1 M H₂O₂; the solution etches away the Cu substrate (25 μm) underneath the CVD graphene within 10 min. The graphene sample was thoroughly cleaned by replacing the etching solution with distilled water. The substrate with the transferred graphene was placed on a hot plate and kept at 35 °C for 10 min, followed by baking at 200 °C for 20 min. After the substrate with the graphene was cooled down to ~60 °C, it was exposed to acetone vapors for 5 minutes and then submerged into a hot acetone bath for ~15 minutes to remove the cellulose acetate.

2.2. PMMA graphene transfer

As-grown monolayer CVD graphene was first spin coated with a

Table 1Comparison of several parameters of different graphene transfer methods.

comparison of several parameters of university graphene transfer methods.						
Graphene transfer method	Approximate time for one transfer	Cost	On/off ratio FET ($V_G = 30\ V$)	Contamination	Comment	Ref.
Conventional wet transfer (PMMA/Fe ³⁺)	1–2 days	High	2.2	Magnetic, PMMA	Light sensitive	[14]
Clean lifting transfer (Static charge/Fe3 ⁺)	2 h	High	2.4	Magnetic	High voltage	[15]
Polymer-free transfer (IPA/(NH ₄) ₂ S ₂ O ₈)	4 h	Medium	N/A	No	Low yield	[30]
Cellulose acetate transfer (Cellulose/H ₂ O ₂ /HCl)	1 h	Low	3.5	No	High throughput	Present study

PMMA solution (950 PMMA A4, MicroChem, 10% by volume dissolved in chlorobenzene) at 2000 rpm. The spin-coated thin film was kept at room temperature overnight inside a clean petri dish. The graphene on the uncoated side was etched away by oxygen plasma as described in section 2.1. Then the PMMA/Graphene/Cu sample was placed on the surface of FeCl₃ solution (0.5 M) to etch away the Cu substrate (thickness 25 μm; typical etching time 60 min). After the Cu was removed, the etching solution was replaced with clean water by repeatedly flowing out the waste solution and flowing in clean water until neutral pH was reached. The substrate with the graphene was transferred to a hot plate and kept at 35 °C for 10 min. After this step the temperature was increased and maintained at 200 °C for 20 min. The substrate with the graphene was cooled down to ~60 °C and kept in a hot acetone bath overnight to remove the PMMA.

2.3. Raman spectroscopy and mapping

Raman spectra and mapping of CVD graphene were recorded with a Nicolet Almega XR Dispersive Raman microscope using laser excitation of 532 nm at 25% power. The laser spot size is around 1 μm with a 50 x objective lens. The Raman mapping area for all samples is 20 $\mu m \times$ 18 μm , with a step size of 1 μm in both x and y directions.

2.4. Atomic force microscopy (AFM)

AFM images were collected in a tapping mode with Digital Instruments, Nanoscope IIIA.

2.5. X-ray photoelectron spectroscopy (XPS)

XPS of transferred CVD graphene on 300 nm SiO $_2$ /Si substrates was carried out with a Kratos AXIS ULTRADLD XPS system equipped with Al K α monochromated X-ray source and a 165 mm mean radius electron energy hemispherical analyzer. Vacuum pressure was kept below 3 \times 10 $^{-9}$ torr during the acquisition. The high-resolution scans were run using a power of 300 W, 20 pass energy and a step size of 0.05 eV. A low-energy electron flood from a filament was used for charge neutralization. The size slot for the XPS is 300 μ m \times 700 μ m. The peak fits consist of Lorentzian and Gaussian distributions.

2.6. Fabrication of field effect transistors (FETs)

Drain and source electrodes (10 nm Cr/100 nm Au) were evaporated by an E-beam evaporator onto 300 nm SiO₂/Si substrates with a shadow mask. After that, the as-grown monolayer CVD graphene was transferred onto the pre-patterned substrates by the conventional PMMA transfer and CAT methods, respectively. The channel dimensions of all graphene devices are 0.25 mm (length) \times 1 mm (width). No photolithography was employed to exclude the effect of photoresist residues on the electronic

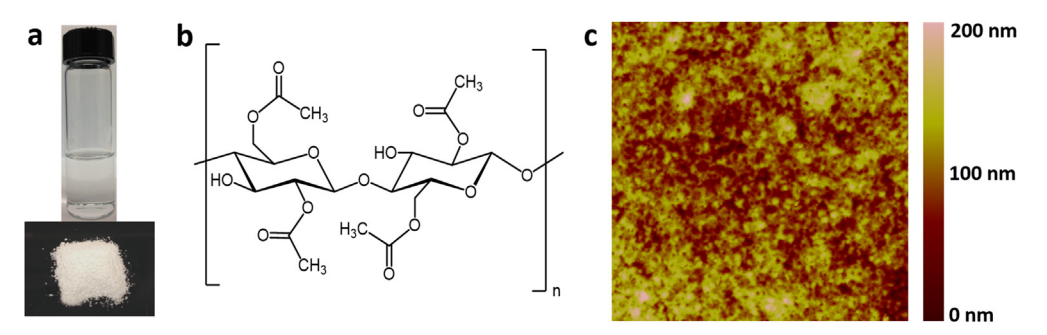


Fig. 1. (a) Photographs of a cellulose acetate powder (bottom) and a cellulose acetate solution in acetone (top). (b) Structure of cellulose acetate. (c) AFM image of a spin-coated cellulose acetate thin film on top of as-grown CVD graphene. (A colour version of this figure can be viewed online.)

properties of the transferred graphene samples. Thermal annealing at 200 $^{\circ}C$ in vacuum (5 \times 10^{-7} torr) for 2 h was performed to remove atmospheric dopants and bring the Dirac point in the vicinity of 0 V.

3. Results and discussion

3.1. Description of the graphene transfer method

In this work, we employed cellulose acetate as a holding layer to protect graphene during the transfer process because of its low cost, excellent draping qualities and environmentally friendly properties. Cellulose acetate, an acetylated derivative of the naturally abundant and sustainable polymer cellulose, can be dissolved in acetone and, when spin-coated on a flat surface, it gives a continuous thin and flexible film (Fig. 1). Cellulose acetate has a long history of application in a number of industrial fields. It has been used as the film base in photography [31], as a substrate for magnetic tape [32], and as a component in household fabrics [33], among other applications. Thus, a mature and comprehensive system to produce, transport and stock cellulose acetate has already been built.

For the graphene transfer, a thin layer of cellulose acetate film is first spin-coated on top of the graphene film grown on Cu or Ni, as shown in Fig. 2a. The cellulose acetate film adheres strongly to the graphene surface and protects it from the surface tension of the

etching solution after the Cu or Ni are removed. The metal substrate (Cu) is etched with an $H_2O_2/HCl/H_2O$ solution. For the etching the central batch reactor (Fig. 2) is filled with a fresh $H_2O_2/HCl/H_2O$ solution and the cellulose acetate/graphene/copper sample is placed on the surface of the etching solution. The etching occurs through the following chemical reaction:

$$H_2O_2 + 2HCl + Cu \rightarrow CuCl_2 + 2H_2O$$

After the copper is completely etched away, fresh water is introduced into the central reactor from the inlet tank and the waste solution is extracted from the outlet tank at the same rate using peristaltic pumps, thus converting the system into a continuous tank reactor. After the pH of the solution inside the reactor approaches that of pure water, the target substrate is positioned onto the bottom of the central reactor through a slit designed between the inlet tank and the central reactor. In the next step, the water is drained out from the outlet tank at a slow rate allowing the cellulose acetate/graphene to transfer down onto the substrate.

Alternatively, the floating cellulose acetate coated graphene can be lifted out from the pure water bath with the target substrate. Next, the cellulose acetate/graphene/target substrate is transferred to a hot plate and kept at 35 °C for 10 min to remove large water droplets trapped between the graphene film and the substrate. The temperature is then increased to 200 °C and maintained for 20 min to enhance the contact between graphene and the substrate. The

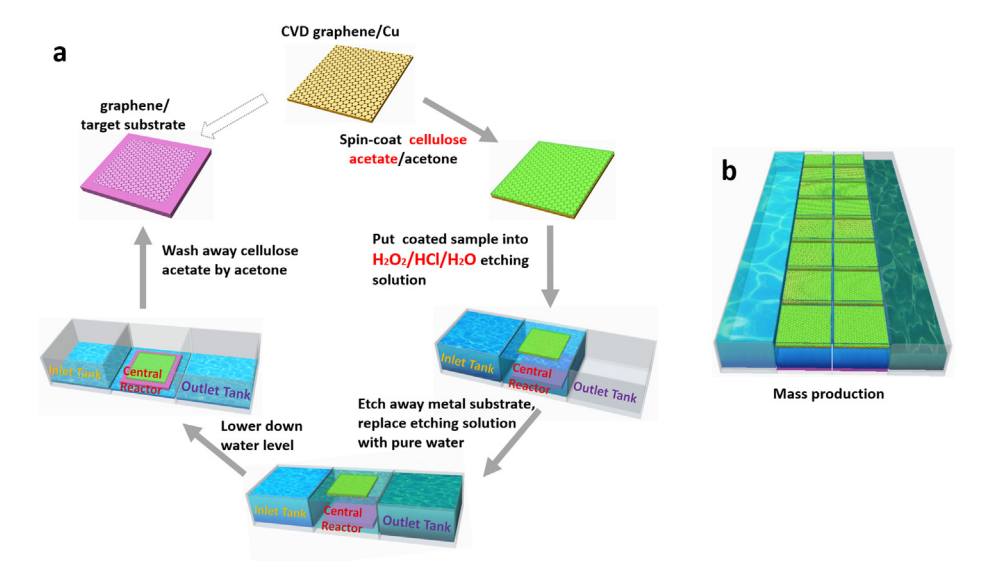


Fig. 2. Schematic illustration of (a) the CAT method and (b) the reactor for simultaneous transferring graphene onto multiple substrates for industrial applications. (A colour version of this figure can be viewed online.)

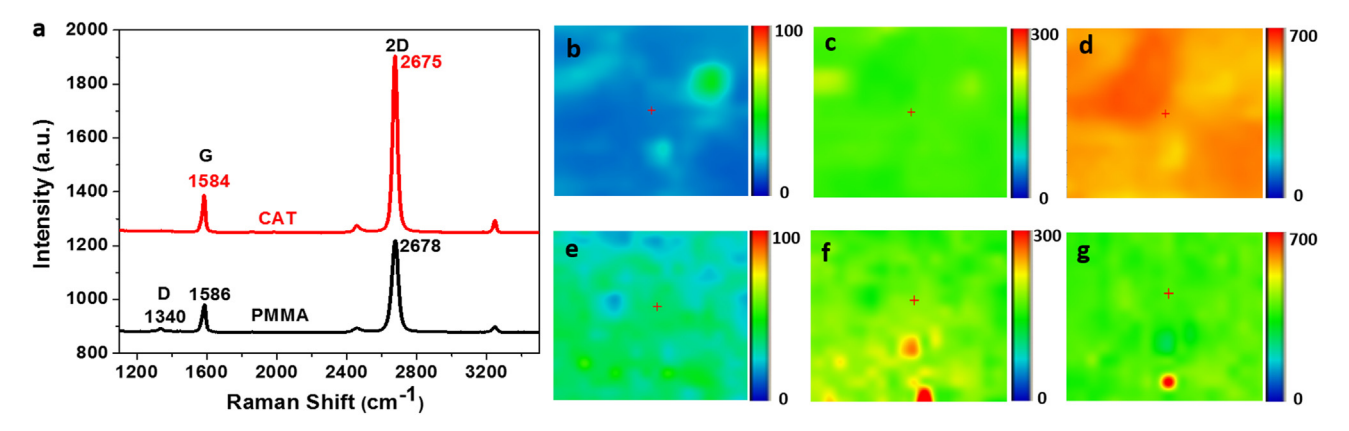


Fig. 3. (a) Raman spectra of single layer CVD graphene transferred by the CAT and PMMA methods. (b-d) Raman intensity maps of D, G and 2D peaks, respectively, for CAT-graphene on a SiO₂/Si substrate. (e-g) Raman intensity maps of D, G and 2D peaks, respectively, for PMMA-graphene on a SiO₂/Si substrate. (A colour version of this figure can be viewed online.)

final step of the transfer process is removing the cellulose film, which is dissolved in hot acetone vapors for 5 min. The substrate with the graphene is then submerged into hot acetone to completely remove the cellulose acetate. The process can be easily scaled to simultaneously conduct the graphene transfer on multiple substrates as illustrated in Fig. 2b.

3.2. Characterization of the transferred graphene

In order to systematically investigate the quality of the CAT graphene and compare it with the conventional wet transfer method, various characterization tools were employed. Raman spectroscopy is a powerful and sensitive technique to characterize the quality of carbon materials, specifically graphene [34,35]. The appearance of a D peak in the vicinity of 1340 cm⁻¹ generally indicates presence of defects in the sp² carbon network of graphene [34,36]. Other important metrics are the amplitude and spectral shape of the G and 2D peaks, observed in the vicinity of 1580 cm⁻¹ and 2700 cm⁻¹, respectively, which can be utilized to characterize the quality of graphene and the number of graphene layers [35]. For example, because the 2D peak is sensitive to long range order, higher peak intensity is an indication of higher crystalline quality of the single layer graphene [35]. Fig. 3a compares representative Raman spectra of graphene samples transferred by the CAT and PMMA-assisted methods. The CAT graphene typically gives a Raman spectrum with little or no D peak as compared to the obvious D peak present in the Raman spectrum of graphene after the PMMA transfer. This is an indication of a much smaller concentration of defects in the CAT-graphene. G and 2D peaks are well pronounced in both samples, but the 2D to G peak ratio is approximately 2 times higher for the CAT graphene film confirming its higher quality as compared to the conventional wet transfer method. Moreover, the slight blue shift of the position of G peak and 2D peak of PMMA-graphene compared to CAT-graphene indicates that p type dopants were introduced [37,38], most likely due to PMMA residues [29].

In addition to the evaluation of the individual spectra (Fig. 3a) we conducted a statistical comparison of the quality of the graphene films by collecting Raman maps of 20 $\mu m \times 18~\mu m$ areas. The D, G and 2D peak maps are shown in Fig. 3b—d for the CAT-graphene and Fig. 3e—g for the PMMA transferred graphene, respectively. Comparison of the D peak maps (Fig. 3b and e) shows that most of the area in the case of CAT-graphene is defect free and less than 10% of the area displays a relatively small D peak, which confirms that the CAT method yields graphene with significantly lower defect density as compared to the conventional wet transfer

method. Fig. 3c and 3f show similar amplitudes of the G peak across both graphene samples, while the average amplitude of the 2D peak in CAT-graphene sample is about 2 times higher than that in PMMA-graphene, which indicates that the CAT method preserves the quality of single layer CVD graphene. Overall, Raman spectroscopy shows that the CAT-graphene is almost defect free (Fig. 3b), displaying a relatively uniform large intensity 2D peak (Fig. 3d), while the PMMA-transferred graphene displays a prominent D peak throughout the mapped surface (Fig. 3e) accompanied with a lower intensity 2D peak (Fig. 3g).

Atomic force microscopy (AFM) was employed to characterize the surface cleanliness and morphology of the graphene transferred by both methods. As shown in Fig. 4a, graphene transferred by the CAT method shows a very clean and relatively uniform surface with an average roughness (Ra) of 0.4 nm. The AFM images revealed the presence of wrinkles with an average height of ~1 nm (Fig. 4b). The majority of the wrinkles presumably originate from the growth process of CVD graphene (formed during the cool down step) [13]. Some wrinkles may be introduced during the transfer process by mechanical manipulation or thermal expansion due to temperature change. We note that even scotch tape exfoliated graphene may have wrinkles [39]. In contrast, the surface of the PMMA-assisted graphene is covered with a polymer residue (Fig. 4d) with a typical height of the impurities being >5 nm and an average roughness of 1 nm; 2.5 times higher than in CAT-graphene (Fig. 4e). The cleanness of the CAT-graphene is further confirmed by XPS spectroscopy. Fig. 4g and 4h display the typical C1s core spectra of graphene samples transferred by the CAT and PMMA methods. The CAT-graphene gives rise to a narrow C1s peak with a major contribution from sp² hybridized C atoms (284.4 eV) and a shoulder at 285.3 eV associated with sp³ carbon presumably due to edges and defects [23]. The C1s spectrum of the PMMA transferred graphene is broad and it can be deconvoluted to five peaks. In addition to the sp² hybridized (284.4 eV) and sp³ hybridized (285.1 eV) carbon peaks, there is a significant contribution from C-O species associated with the PMMA residue (C-O at 286.5 eV. C=O at 287.5 eV and C-C=O at 289 eV) [23].

In order to compare the electronic transport properties of the CVD graphene prepared by the CAT and PMMA transfers, graphene-based back gated field effect transistors (FETs) were fabricated on 300 nm SiO $_2$ /Si substrates with pre-patterned Cr/Au electrodes. Relatively large dimensions of graphene devices with a channel length of 0.25 mm and channel width of 1 mm were fabricated in order to avoid contamination with resist residues during the photolithography or the e-beam lithography processes. Prior to measurements the devices were annealed at 200 $^{\circ}$ C in vacuum for

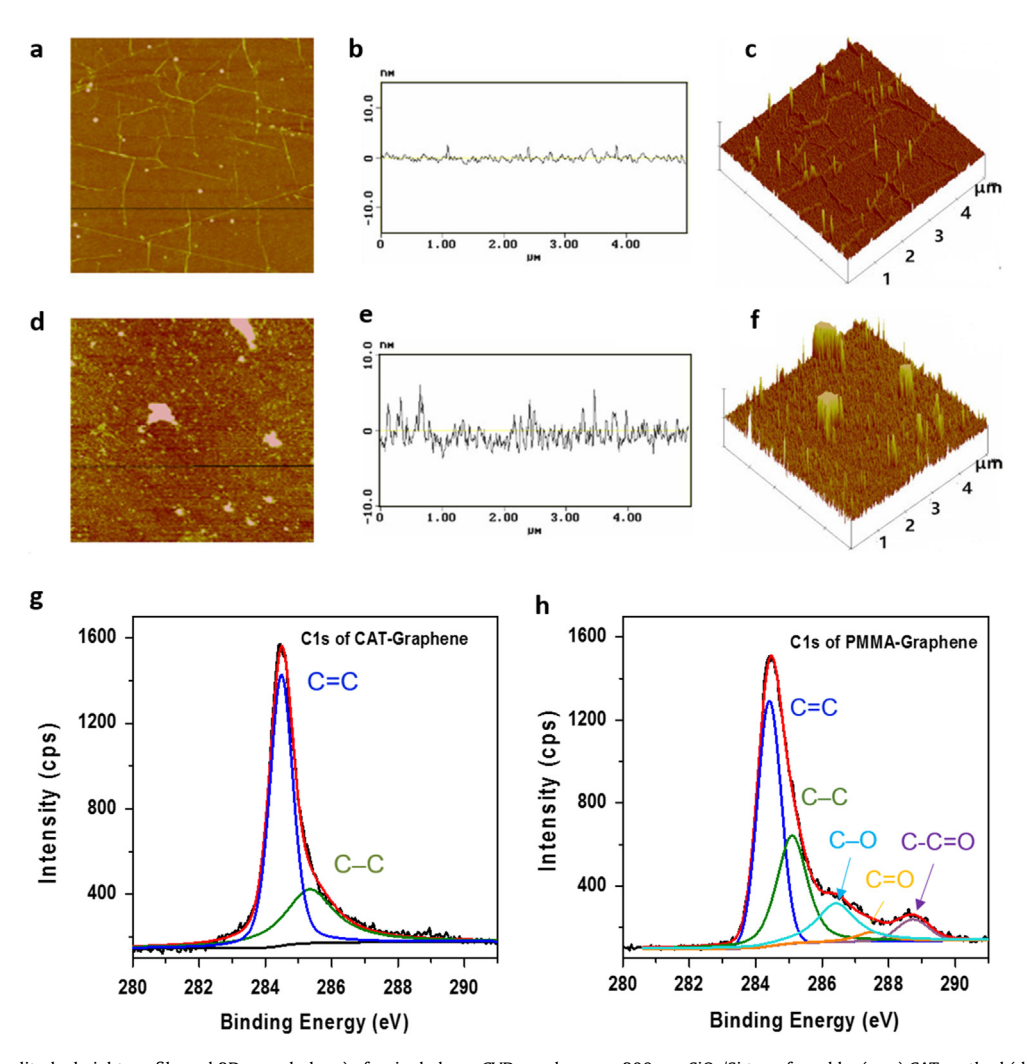


Fig. 4. AFM images (amplitude, height profile and 3D-morphology) of a single layer CVD graphene on 300 nm SiO₂/Si transferred by (a–c) CAT method (d–f) PMMA method. C1s core spectra of single layer graphene transferred by (g) CAT and (h) PMMA method. The peak fits consist of Lorentzian and Gaussian distributions. (A colour version of this figure can be viewed online.)

2 h. Fig. 5a shows the transport characteristics of the corresponding FET devices. The FET fabricated with the CAT-graphene shows sharper and more symmetric transport characteristics in comparison with the PMMA-transferred graphene device. The hole and electron mobilities extracted from the linear range for CAT transferred graphene are 1695 cm 2 V $^{-1}$ s $^{-1}$ and 1675 cm 2 V $^{-1}$ s $^{-1}$,

respectively, significantly higher than those obtained for the PMMA transferred graphene (450 cm 2 V $^{-1}$ s $^{-1}$ for holes and 380 cm 2 V $^{-1}$ s $^{-1}$ for electrons).

The larger difference between the hole and electron mobilities for the PMMA transferred graphene device indicates an asymmetry of scattering for the two types of carriers, which may be caused by

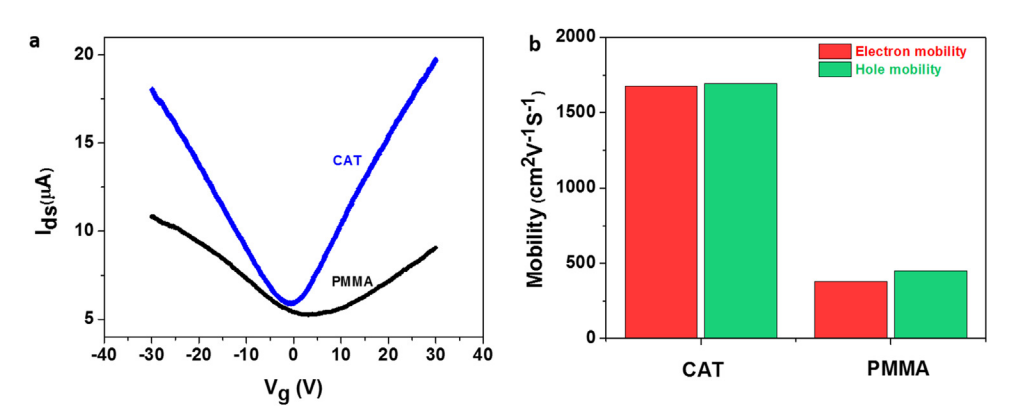


Fig. 5. FET characterization of graphene transferred onto 300 nm SiO₂/Si substrates. (a) Drain-source current vs gate voltage of the FET devices. (b) Comparison of the mobilities of the large size CAT-graphene and PMMA-graphene devices. (A colour version of this figure can be viewed online.)

the residual contaminants (Fe³⁺ and PMMA). In principle, higher mobility values are reported in the literature for some CVD graphene samples [13] [17], however those reports typically utilize graphene channels of microscopic (<10 μ m) dimensions, while the current study is conducted with millimeter scale devices in which high mobility is much more difficult to achieve.

Compared with the PMMA transferred method, the cellulose assisted transfer introduces much fewer residues, and magnetic impurities, which largely conserves the transport properties of the original CVD graphene and thus obtain higher mobility devices.

4. Conclusion

In summary, a novel cellulose acetate assisted graphene transfer method (CAT) suitable for both academic and industrial applications is presented in this paper. The CAT system not only solves the problems associated with PMMA and magnetic material contaminations introduced by most transfer methods, but also largely reduces the transfer cost and time, while providing a very convenient system for precise and efficient transfer of clean graphene on various substrates. We demonstrated the advantages and high quality of the CAT- graphene by means of Raman spectroscopy, Atomic Force Microscopy, and X-ray photoelectron spectroscopy. Macroscopic size single-layer graphene-based field effect transistors were fabricated and the extracted mobilities were about 2 times higher for the CAT-graphene devices than those for the PMMA-graphene devices. This method has potential to facilitate graphene related research and expedite the commercialization of CVD graphene.

Acknowledgements

This work was funded by NSF under contract DMR-1305724. XPS measurements were performed with an instrument acquired with NSF support under contract DMR-0958796. We would like to thank Dr. Ruoxue Yan for valuable discussions.

References

- [1] P.R. Wallace, The band theory of graphite, Phys. Rev. 71 (9) (1947) 622-634.
- [2] K.S. Novoselov, A.K. Geim, S.V. Morozov, D. Jiang, Y. Zhang, S.V. Dubonos, et al., Electric field effect in atomically thin carbon films, Science 306 (2004) 666–669.
- [3] C. Berger, Z. Song, T. Li, X. Li, A.Y. Ogbazghi, R. Feng, et al., Ultrathin epitaxial graphite: 2D electron gas properties and a route toward graphene-based nanoelectronics, J. Phys. Chem. B 108 (52) (2004) 19912–19916.
- [4] Z.H. Chen, Y.M. Lin, M.J. Rooks, P. Avouris, Graphene nano-ribbon electronics, Phys. E 40 (2) (2007) 228–232.
- [5] C.-H. Liu, Y.-C. Chang, T.E. Norris, Z. Zhong, Graphene photodetectors with ultra-broadband and high responsivity at room temperature, Nat. Nanotechnol. 9 (2014) 273–278.
- [6] F. Torrisi, T. Hasan, W.P. Wu, Z.P. Sun, A. Lombardo, T.S. Kulmala, et al., Inkjet-printed graphene electronics, ACS Nano 6 (4) (2012) 2992–3006.
- [7] E. Bekyarova, S. Niyogi, S. Sarkar, X. Tian, M. Chen, M.L. Moser, et al., Stereo-chemical effect of covalent chemistry on the electronic structure and properties of the carbon allotropes and graphene surfaces, Synth. Met. 210 (2015) 80–84.
- [8] M. Chen, X. Tian, W. Li, E. Bekyarova, G. Li, M. Moser, et al., Application of organometallic chemistry to the electrical interconnection of graphene nanoplatelets, Chem. Mater. 28 (7) (2016) 2260–2266.
- [9] R.R. Nair, M. Sepioni, I.-L. Tsai, P.O. Lehtinen, J. Keinonen, A.V. Krasheninnikov, et al., Spin-half paramagnetism in graphene induced by point defects, Nat. Phys. 8 (2012) 199–202.
- [10] Y. Li, H. Yuan, A. von dem Bussche, M. Creighton, R.H. Hurt, A.B. Kane, et al., Graphene microsheets enter cells through spontaneous membrane penetration at edge asperities and corner sites, Proc. Natl. Acad. Sci. U. S. A. 110 (30) (2013) 12295—12300.
- [11] F. Guo, G. Silverberg, S. Bowers, S. Kim, D. Datta, V. Shenoy, et al., Graphene-based environmental barriers, Environ. Sci. Technol. 46 (14) (2012)

- 7717-7724.
- [12] T. Zhang, H. Chang, Y. Wu, P. Xiao, N. Yi, Y. Lu, et al., Macroscopic and direct light propulsion of bulk graphene material, Nat. Photonics 9 (7) (2015)
- [13] X.S. Li, W.W. Cai, J.H. An, S. Kim, J. Nah, D.X. Yang, et al., Large-area synthesis of high-quality and uniform graphene films on copper foils, Science 324 (5932) (2009) 1312–1314.
- [14] X. Liang, B.A. Sperling, I. Calizo, G. Cheng, C.A. Hacker, Q. Zhang, et al., Toward clean and crackless transfer of graphene, ACS Nano 5 (11) (2011) 9144–9153.
- [15] D. Wang, I. Huang, P. Ho, S. Li, Y. Yeh, D. Wang, et al., Clean-lifting transfer of large-area residual-free graphene films, Adv. Mater. 25 (32) (2013) 4521–4526.
- [16] T. Kobayashi, M. Bando, N. Kimura, K. Shimizu, K. Kadono, N. Umezu, et al., Production of a 100-m-long high-quality graphene transparent conductive film by roll-to-roll chemical vapor deposition and transfer process, Appl. Phys. Lett. 102 (2) (2013) 023112.
- [17] L. Gao, G.X. Ni, Y.P. Liu, B. Liu, A.H. Castro Neto, K.P. Loh, Face-to-face transfer of wafer-scale graphene films, Nature 505 (7482) (2014) 190–194.
- [18] S.J. Kim, T. Choi, B. Lee, S. Lee, K. Choi, J. Park, et al., Ultraclean patterned transfer of single-layer graphene by recyclable pressure sensitive adhesive films, Nano Lett. 15 (5) (2015) 3236–3240.
 [19] X.S. Li, Y.W. Zhu, W.W. Cai, M. Borysiak, B.Y. Han, D. Chen, et al., Transfer of
- [19] X.S. Li, Y.W. Zhu, W.W. Cai, M. Borysiak, B.Y. Han, D. Chen, et al., Transfer of large-area graphene films for high-performance transparent conductive electrodes, Nano Lett. 9 (12) (2009) 4359–4363.
- [20] Y. Wu, Y. Lin, A.A. Bol, K.A. Jenkins, F. Xia, D.B. Farmer, et al., High-frequency, scaled graphene transistors on diamond-like carbon, Nature 472 (7341) (2011) 74-78.
- [21] Q. Yu, L.A. Jauregui, W. Wu, R. Colby, J. Tian, Z. Su, et al., Control and characterization of individual grains and grain boundaries in graphene grown by chemical vapour deposition, Nat. Mater. 10 (6) (2011) 443–449.
- [22] Y. Wu, K.A. Jenkins, A. Valdes-Garcia, D.B. Farmer, Y. Zhu, A.A. Bol, et al., State-of-the-art graphene high-frequency electronics, Nano Lett. 12 (6) (2012) 3062–3067
- [23] Y. Lin, C. Lu, C. Yeh, C. Jin, K. Suenaga, P. Chiu, Graphene annealing: how clean can it be? Nano Lett. 12 (1) (2011) 414–419.
- [24] H. Park, P.R. Brown, V. Bulovic, J. Kong, Graphene as transparent conducting electrodes in organic photovoltaics: studies in graphene morphology, hole transporting layers, and counter electrodes, Nano Lett. 12 (1) (2012) 133–140.
- [25] A. Ambrosi, M. Pumera, The CVD graphene transfer procedure introduces metallic impurities which alter the graphene electrochemical properties, Nanoscale 6 (1) (2014) 472–476.
- [26] S. Bae, H. Kim, Y. Lee, X.F. Xu, J.S. Park, Y. Zheng, et al., Roll-to-roll production of 30-inch graphene films for transparent electrodes, Nat. Nanotechnol. 5 (8) (2010) 574–578.
- [27] Y. Lee, K. Tu, C. Yu, S. Li, J. Hwang, C. Lin, et al., Top laminated graphene electrode in a semitransparent polymer solar cell by simultaneous thermal annealing/releasing method, ACS Nano 5 (8) (2011) 6564–6570.
- [28] J.W. Suk, A. Kitt, C.W. Magnuson, Y. Hao, S. Ahmed, J. An, et al., Transfer of CVD-grown monolayer graphene onto arbitrary substrates, ACS Nano 5 (9) (2011) 6916–6924.
- [29] A. Pirkle, J. Chan, A. Venugopal, D. Hinojos, C.W. Magnuson, S. McDonnell, et al., The effect of chemical residues on the physical and electrical properties of chemical vapor deposited graphene transferred to SiO₂, Appl. Phys. Lett. 99 (12) (2011) 122108.
- [30] W.H. Lin, T.H. Chen, J.K. Chang, J.I. Taur, Y.Y. Lo, W.L. Lee, et al., A direct and polymer-free method for transferring graphene grown by chemical vapor deposition to any substrate, ACS Nano 8 (2) (2014) 1784–1791.
- [31] JS Machell, ID Sand, inventors; Light sensitive silver halide element with cellulose ester film base. US patent US5288715 A. 1994.
- [32] BRA Von, inventor Magnetic recording tape and method of making same. US patent US 2711901 A. 1955.
- [33] JC Chen, KJ Soden, inventors; Anti-adhesion cellulose acetate wound dressing. US patent US 6500539 B1. 2002.
- [34] M.S. Dresselhaus, A. Jorio, M. Hofmann, G. Dresselhaus, R. Saito, Perspectives on carbon nanotubes and graphene raman spectroscopy, Nano Lett. 10 (3) (2010) 751–758.
- [35] A.C. Ferrari, D.M. Basko, Raman spectroscopy as a versatile tool for studying the properties of graphene, Nat. Nanotechnol. 8 (4) (2013) 235–246.
- [36] A.C. Ferrari, J.C. Meyer, V. Scardaci, C. Casiraghi, M. Lazzeri, F. Mauri, et al., Raman spectrum of graphene and graphene layers, Phys. Rev. Lett. 97 (2006) 187401–187404.
- [37] S. Pisana, M. Lazzeri, C. Casiraghi, K.S. Novoselov, A.K. Geim, A.C. Ferrari, et al., Breakdown of the adiabatic Born-Oppenheimer approximation in graphene, Nat. Mater. 6 (2007) 198–201.
- [38] A. Das, S. Pisana, B. Chakraborty, S. Piscanec, S.K. Saha, U.V. Waghmare, et al., Monitoring dopants by Raman scattering in an electrochemically top-gated graphene transistor, Nat. Nanotechnol. 3 (2008) 210–215.
- [39] S.V. Morozov, K.S. Novoselov, M.I. Katsnelson, F. Schedin, L.A. Ponomarenko, D. Jiang, et al., Strong suppression of weak localization in graphene, Phys. Rev. Lett. 97 (2006) 016801.